npj | climate and atmospheric science

Article

Published in partnership with CECCR at King Abdulaziz University

https://doi.org/10.1038/s41612-025-01163-0

Challenges in assessing Fire Weather changes in a warming climate

Check for updates

Aurora Matteo[1], Ginés Garnés-Morales[2], Alberto Moreno[2], Andreia F. S. Ribeiro[3], Cesar Azorin-Molina[4], Joaquín Bedia[5], Francesca Di Giuseppe[6], Robert J. H. Dunn[7], Sixto Herrera[5], Antonello Provenzale[8,9], Yann Quilcaille[10], Miguel Ángel Torres-Vázquez[2,11] & Marco Turco[2] ✉

The Canadian Fire Weather Index (FWI), widely used to assess wildfire danger, typically relies on noon-specific meteorological data. However, climate models often provide only daily aggregated values, posing a challenge for accurate FWI calculations. We evaluated daily approximations for FWI95d—the annual count of extreme fire-weather days—against the standard noon-based method (1980–2023). Our findings reveal that noon-based FWI95d show a global increase of ~65% (11.66 days over 44 years). In contrast, daily approximations tend to overestimate these trends by 5–10%, with combinations involving minimum relative humidity showing the largest divergences. Globally, up to 15 million km²—particularly in the western United States, southern Africa, and parts of Asia—exhibit significant overestimations. We recommend (i) prioritizing the inclusion of sub-daily meteorological data in future climate model intercomparison projects to enhance FWI accuracy, and (ii) adopting daily mean approximations as the least-biased alternative if noon-specific data are unavailable.

The Canadian Fire Weather Index (FWI) is one of the most widely used indicators for evaluating how climatic and meteorological conditions influence wildfire spread once ignition occurs[1,2]. Relying solely on meteorological inputs—2-meter air temperature, 2-meter relative humidity, 24-hour precipitation, and 10-meter wind speed—the FWI was calibrated for fire weather conditions at the point of maximum air temperature. The FWI formulation uses meteorological data recorded at local noon, as it is intended to represent fire danger at its midafternoon peak (around 16:00); this timing was chosen because noon weather conditions show the strongest correlation with fine fuel moisture levels and fire activity observed later in the day[3]. However, noon-specific observations are often unavailable in climate model outputs commonly shared through the Earth System Grid Federation (ESGF; https://esgf.llnl.gov/; last accessed 16 January 2025). As a result, researchers have relied on approximations using daily-averaged meteorological data[4].

ref. 5 first demonstrated systematic biases in FWI when using daily means for the Iberian Peninsula, advising the use of noon-specific data for climate projections. ref. 6 extended this to Europe and found that combining maximum air temperature and minimum relative humidity was reliable in representing fire danger. More recently, ref. 7 produce a global fire weather index dataset based on simulations performed under the Coupled Model Intercomparison Project Phase 6 (CMIP6) and provided sensitivity analysis of fire weather indices to relative humidity proxies, comparing future projections of the FWI when using either minimum or mean relative humidity values, as derived from global climate models. Their findings indicated that replacing minimum relative humidity with mean relative humidity consistently reduced FWI during fire seasons, regardless of the time period (1994–2014 or 2081–2100). This suggests that the choice of humidity metric may not drastically alter relative changes in FWI over time. However, they do not assess the influence of other approximations (e.g., mean or maximum temperature instead of noon values) and do not check for differences in trend. As we will see, the differences introduced by daily approximations may not be constant but accumulate over time, leading to overestimated projections of future fire weather danger. Thus, relatively simple and widely used methods for future projections, like the delta method, cannot fully compensate for these differences because it corrects for the mean biases but

[1]Department of Earth Sciences, University of Pisa, Pisa, Italy. [2]Department of Physics, Regional Campus of International Excellence (CEIR) Campus Mare Nostrum, University of Murcia, Murcia, Spain. [3]Department of Compound Environmental Risks, Helmholtz Centre for Environmental Research - UFZ, Leipzig, Germany. [4]Centro de Investigaciones sobre Desertificación, Consejo Superior de Investigaciones Científicas (CIDE, CSIC-UV-Generalitat Valenciana), Climate, Atmosphere and Ocean Laboratory (Climatoc-Lab), Moncada, Valencia, Spain. [5]Departamento de Matemática Aplicada y Ciencias de la Computación (MACC), Universidad de Cantabria, Santander, Spain. [6]European Center for Medium-range Weather Forecast (ECMWF), Reading, UK 7Met Office Hadley Centre, Exeter, UK. [7]Met Office Hadley Centre, Exeter, UK. [8]Institute of Geosciences and Earth Resources, CNR, Torino, Italy. [9]Cima Research Foundation, Savona, Italy. [10]Institute for Atmospheric and Climate Science, Department of Environmental Systems Science, ETH Zurich, Zurich, Switzerland. [11]Universidad de Alcalá, Environmental Remote Sensing Research Group, Department of Geology, Geography and the Environment, Calle Colegios 2, Alcalá de Henares, Spain. ✉e-mail: marco.turco@um.es

does not account for diverging trends. That is, it remains still unclear how much deviations the approximations based on daily values may introduce.

Answering this question could have significant implications for estimates of changes in landscape flammability, underpinning a substantial body of recent research (e.g., refs. 2,7–9). This is particularly relevant as global analyses indicate that high FWI conditions have become increasingly frequent, prolonged, and severe under ongoing greenhouse gas emissions[10].

Most studies analysing the projected changes under anthropogenic climate forcings have relied on daily aggregated variables, likely modifying the expected trends. Another concern is that, in the absence of a consensus on the best approach, many studies have adopted different methodological approaches (e.g., substituting air temperature at local noon with maximum or mean daily air temperature), further complicating reproducibility and the comparison of results.

The main aim of this study is to quantify the discrepancy between FWI calculated from daily-averaged versus noon-specific values and to assess the implications this might have. Given that sub-daily data remain sparse in many climate simulations, we address this question through a sensitivity analysis using a reanalysis dataset. Reanalysis datasets integrate observations into atmospheric models to produce physically consistent estimates of climate variables with both spatial and temporal continuity[11]. Such datasets have been widely used in recent fire weather research (e.g., refs. 2,12–14). Among these resources, the Copernicus Emergency Management Service FWI dataset[15]—derived from the ERA5 reanalysis[16] and developed by the European Centre for Medium-Range Weather Forecasts (ECMWF)—has become a benchmark for evaluating fire danger trends (see e.g., ref. 2, and references therein).

In this analysis, we calculate the FWI globally from 1980 to 2023 using various daily approximations and compare these results with the FWI dataset from ref. 15, which is based on sub-daily, noon-specific values. Our goal is to determine whether trends derived from approximate inputs differ significantly from those based on noon-specific inputs, as well as to identify approximation strategies that minimize these discrepancies. We assume that our findings can provide a ballpark estimate of the error associated with climate change projections. Therefore, this analysis will inform the reliability and limitations of future global FWI assessments that rely on climate model outputs lacking midday-specific meteorological data.

Results and discussion

We compare the Fire Weather Index (FWI) dataset (version 4.1)[15] that uses the original FWI definition against four alternative combinations based on daily variables commonly available from climate models—maximum and mean daily air temperature, mean and minimum daily relative humidity, daily precipitation, and daily mean wind speed—to approximate the FWI. Using these daily variables, we generate four different input combinations (C1 to C4), as summarized in Table 1.

The global trend analysis (Fig. 1) shows that the baseline FWI95d (C0) increased by 2.65 days per decade between 1980 and 2023. Over 44 years, that amounts to 11.66 additional days, representing a ~ 65% rise relative to the global average of 18 extreme fire weather days per year. These results align with the findings of ref. 13 and of ref. 2, who similarly observed global increases in extreme fire weather. Specifically, ref. 13 identified decreasing relative humidity and increasing air temperature as key drivers of these trends.

Table 1 | Approaches to estimate the FWI

Comb.	Temp. (°C)	R. Hum. (%)	Precip. (mm)	W. vel. (km h^{-1})
C0	at noon	at noon	24 h*	at noon
C1	DM	DM	24 h	DM
C2	Max	DM	24 h	DM
C3	DM	Min	24 h	DM
C4	Max	Min	24 h	DM

C0 refers to the baseline approach of ref. 15 using the original FWI definition. C1-C4 are the daily-data alternatives replacing noon values. *DM* daily mean, *Max*/*Min* daily maximum/minimum.
*Precipitation is the 24 h accumulation ending at noon for C0 and ending at 00 UTC for the other combinations.

Fig. 1 also highlights that none of the daily approximations (C1–C4; see Table 1) preserve the C0 trend exactly, and all combinations overestimate the trend, ranging from 2.86 to 3.06 days per decade. That equates to an approximate increase of 70–75% over the average FWI95d value (Fig. 1a). In Fig. 1b, we first compute the difference between the FWI95d time series obtained with each daily approximation (C1–C4) and the baseline (C0) and then assess the trend in these difference series. The resulting trends—ranging from 0.22 to 0.39 days per decade—are statistically significant in all cases, indicating that the daily approximations do not preserve the baseline trends and systematically overestimate them.

These results highlight an important caveat for projections of future FWI based on daily-mean meteorological data, as often used in climate models. The reliance on daily averages rather than noon-specific meteorological inputs tends to overestimate the rate of increase in FWI95d globally. It is particularly concerning that combination C4, which uses maximum daily air temperature, minimum daily relative humidity, daily mean wind speed, and daily precipitation, performs the worst among all combinations. C4 is widely accepted as the default approach when subdaily data are unavailable (e.g., refs. 6,7,17). However, Fig. 1 shows that C4 not only overestimates the trend the most but also introduces the largest deviation from the baseline. These findings underscore the urgency of reassessing the methodologies used to approximate the FWI95d when only daily data are available. For instance, reliance on C4 could result in projections that significantly overstate the risks of future extreme fire weather, emphasizing the need to utilize noon-specific meteorological data wherever possible to improve the accuracy of fire weather projections.

While we later discuss our recommendations in detail, we next explore the spatial differences in trends at the grid scale to better understand why these discrepancies arise and where they are most pronounced.

Fig. 2 shows the trends in the FWI95d based on our five combinations (C0-C4). The spatial patterns of the trends are notably similar across all combinations and align with previous studies (e.g., refs. 2,12,13), that identified increasing fire weather in several regions globally.

Specifically, the western United States shows substantial increases in FWI (Fig. 2), underscoring escalating fire weather conditions and wildfire activity in that region -concerns that have been tragically highlighted by recent large-scale fires such as those in the Los Angeles area in January 2025[18–22]. Southern and Central Europe, particularly France, Spain, and Portugal, also exhibit pronounced positive trends[23,24]. Similarly, Central and South America, especially Brazil, display significant positive trends[2]. Africa shows an increase in fire weather, particularly in the central and southern areas. Additionally, significant positive trends are observed in extended areas in Asia, including parts of Turkey and the Middle East. By contrast, India and other parts of South Asia exhibit negative trends, likely tied to increased atmospheric moisture[25] and irrigation patterns[26].

Although the trends in Fig. 2 appear very similar visually, careful analysis is needed to confirm whether daily combinations conserve or alter the reference trend. Fig. 3 shows the trend differences between the four daily approximations (C1–C4) and the baseline (C0) to make it easier to detect divergences in trends. As expected, this highlights regions most sensitive to approximations, revealing potential biases when only daily data are used.

Most grid points do not exhibit statistically significant trends in the differences from the C0 baseline (Fig. 3). In general, daily approximations provide reliable FWI95d trends in many regions. Significant positive trends, where the proxy combinations exceed the baseline, are predominantly observed in the western U.S., southern Africa, localized areas in South America, central Africa, the Iberian Peninsula, western Asia, and eastern Australia. In C3 and C4, additional positive trends appear in western Canada. Few areas show negative trend differences, and these are generally scattered. The extent of these regions varies across combinations (Table 2). It

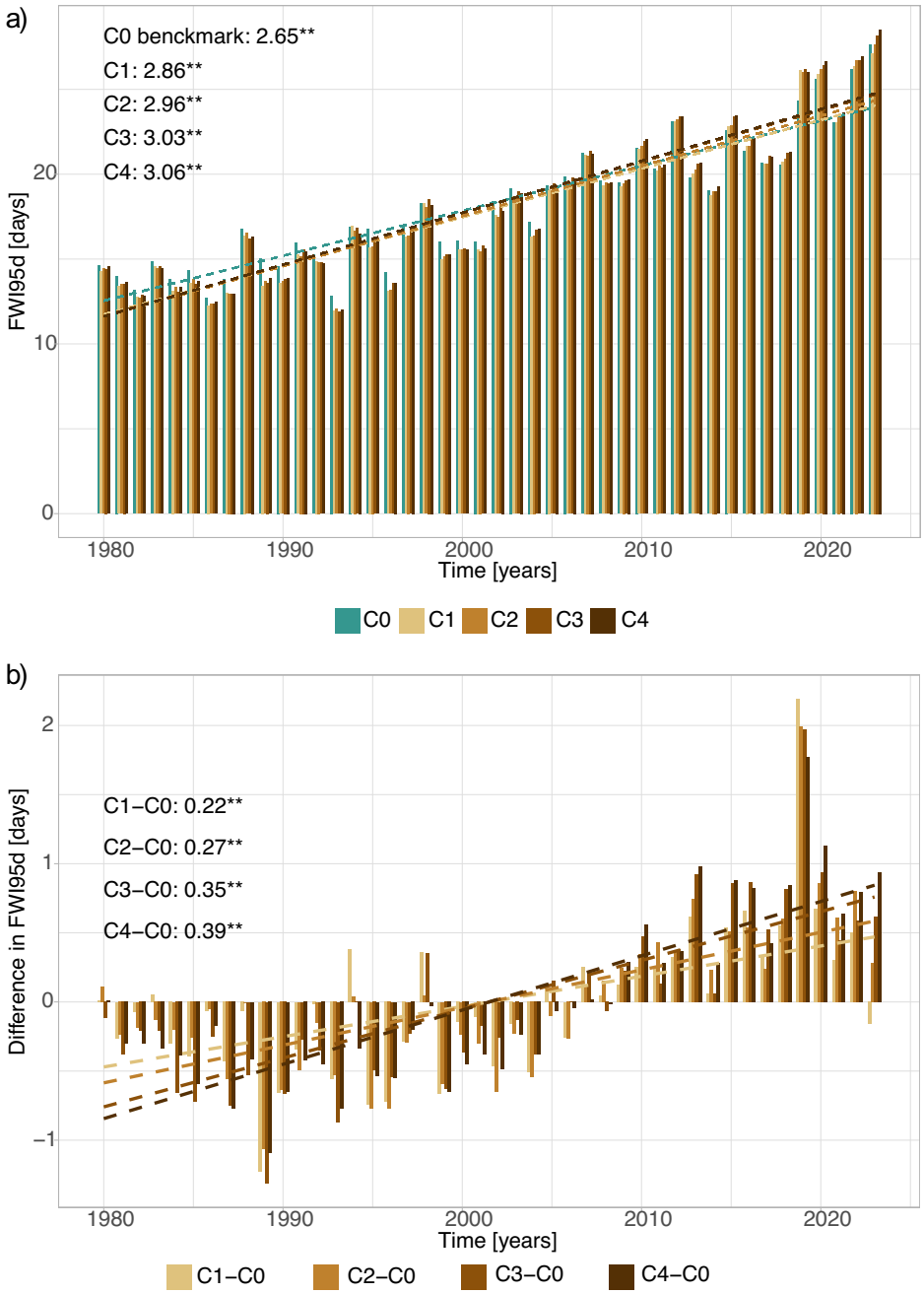

Fig. 1 | Globally averaged FWI95d time series and linear trends from 1980 to 2023. a Time series of FWI95d for different input combinations (C0 to C4). **b** Differences in FWI95d trends for daily approximations (C1 to C4) relative to baseline (C0). Trend estimates (in days per decade) are included, with statistical significance indicated (** for p-value < 0.01).

is lower for C1 and C2, which use mean relative humidity, but higher in C3 and C4, which incorporate minimum relative humidity (Table 2).

Based on the results, relative humidity emerges as pivotal in understanding FWI trends when using daily proxies. Figure. 4 and S2, which isolate each substituted variable, confirm that substituting relative humidity exerts the strongest effect on FWI trends. In contrast, air temperature, wind speed, or precipitation have comparatively minor impacts (Figure. S2). Notably, using mean or minimum RH leads to the largest deviations from C0 in western U.S., southern Africa, eastern parts of central Africa, and eastern Australia (Fig. 4).

To better understand why relative humidity (RH) plays such a central role in determining whether FWI trends are preserved when using approximated RH inputs, we first examine the changes in the key atmospheric variables that drive RH: air temperature and absolute humidity.

As highlighted by ref. 13, the increasing FWI95d globally is primarily driven by rising air temperatures and declining relative humidity. However, although air temperature (T) and RH each influence fire weather, they are not independent: as T increases, RH will decrease unless dew point temperature (Td) also rises. Fig. 5 illustrates spatial T and Td trends, showing where RH becomes disproportionately influential in FWI95d. Trends in T are nearly uniform globally, whereas Td trends exhibit considerable spatial heterogeneity. In particular, Td decreases significantly in the western United States, southern Africa, South America, and parts of Australia.

These decreases are likely driven by a combination of processes reflecting the complex interplay between regional climate dynamics, land use, and the water cycle (e.g., refs. 13,27–29). In semi-arid areas, land–atmosphere feedback constrains moisture availability[30], while deforestation in the Amazon diminishes local evapotranspiration[31]. Such decoupling between T and Td results in sharper RH declines, thereby

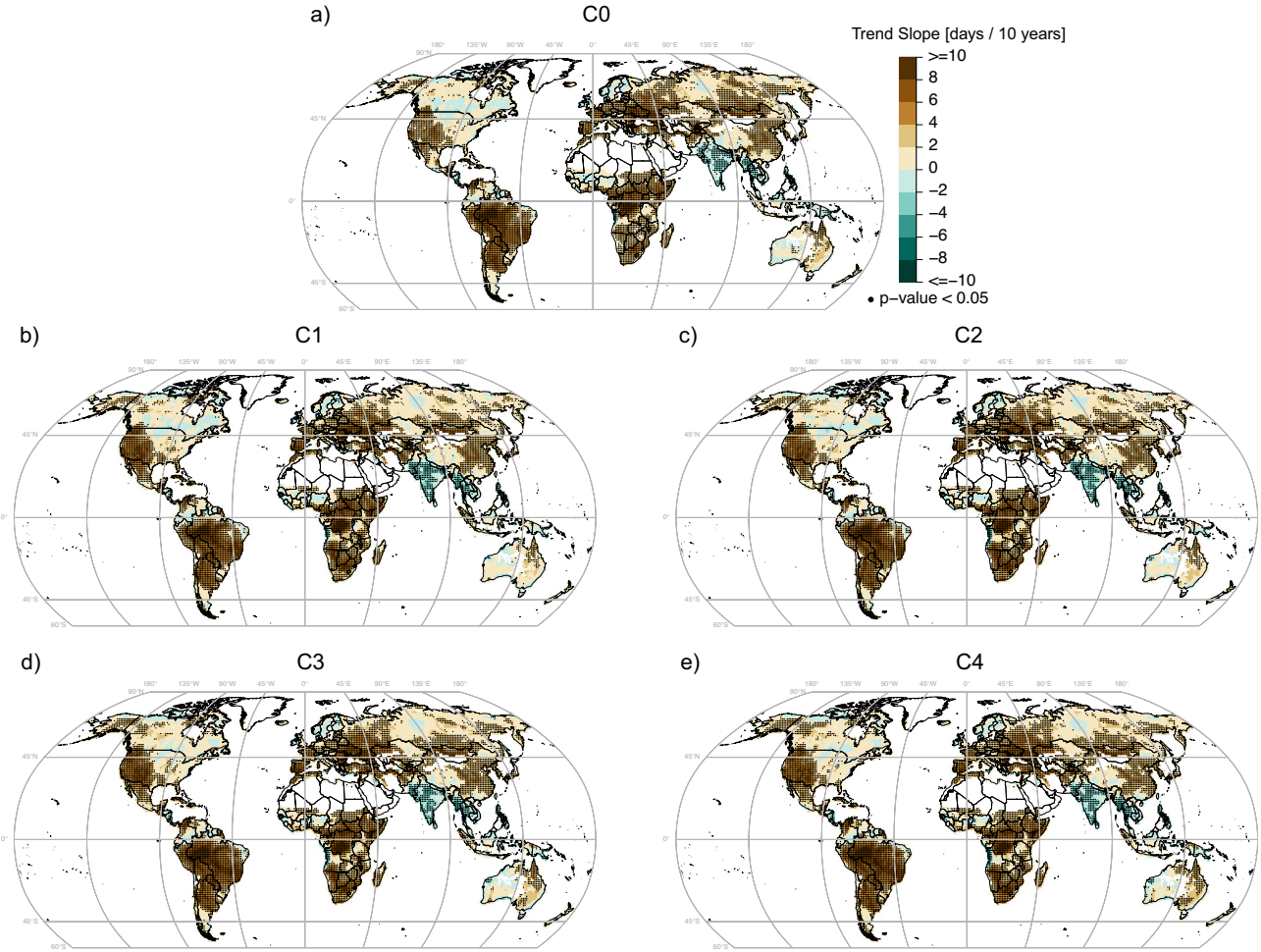

Fig. 2 | Trends in the annual days with FWI values exceeding the 95th percentile (FWI95d) for 1980–2023 for different combinations. a C0, represents the FWI computed using noon-specific variables, and (**b**–**e**) the approximations C1–C4 that use daily mean or min/max values typically available from climate models (Table 1). Regions with significant trends (p-value < 0.05) are outlined with black dots.

amplifying FWI's sensitivity to humidity changes. Likely, in regions where Td is decreasing, RH becomes more sensitive to even minor fluctuations in moisture availability, exacerbating its influence on FWI trends. Such conditions not only amplify the severity of fire weather but also underscore the potential for RH proxies, such as daily mean or minimum values, to misrepresent the actual fire weather dynamics when noon-specific data are unavailable.

To investigate more directly how RH approximations (mean and minimum RH) differ from noon RH during extreme fire danger conditions, we analyse the trends in their differences over FWI95 days (Fig. 6). For each year, we identify days when the FWI exceeds its 95th percentile, compute corresponding RH values (RHnoon, RHmean, and RHmin), and then calculate annual means to evaluate their trends over time. Interestingly, in regions where approximated RH values fail to preserve FWI trends—such as western North America and southeastern Australia—both RHmean and RHmin exhibit steeper negative trends than RHnoon during extreme fire weather days. Despite their different climatological baselines (i.e., RHmean > RHnoon > RHmin), these approximations yield similarly biased FWI trends because of their sharper declines relative to RHnoon.

Moreover, the trend differential between RHmin and RHnoon is locally even greater than between RHmean and RHnoon. This explains why combinations C3 and C4, which use RHmin, produce larger deviations from the reference FWI trend than C1 and C2 (which use RHmean). The key driver of these differences is not the absolute RH values but rather their trend differentials, amplified by the nonlinear dependence of FWI on RH, particularly in increasingly dry and warm conditions. Minimum RH typically occurs during the warmest and driest part of the day, when the atmosphere's capacity to hold moisture is greatest. In regions experiencing declining absolute humidity (i.e., decreasing Td), this effect is magnified, making afternoon RH minima more sensitive to drying conditions. Consequently, higher temperatures combined with reduced moisture availability result in sharper RHmin reductions relative to RHnoon, which occurs earlier in the day, before peak dryness is reached.

Discussion

In our study, we conducted a comprehensive evaluation of the assumptions used in Fire Weather Index (FWI) calculations for climate change applications. Specifically, we assessed the feasibility of approximating noon-specific FWI inputs using daily-mean meteorological data rather than the noon-specific data required by the original FWI definition. We focused on FWI95d, the annual count of days exceeding the local 95th-percentile threshold, for 1980–2023. By comparing the daily approximations against the benchmark by ref. 15, we offered a global perspective of differences and implications for wildfire danger assessment.

Our findings confirm that extreme fire weather is increasing globally: FWI95d has risen by about 65% since 1980, but daily approximations can inflate this figure by an additional 5–10%. This overestimation indicates that future climate projections relying on daily mean data will likely overestimate the rate of global rise in extreme fire weather conditions. This has important implications for the climate modelling community. For future global model experiments, such as the forthcoming Coupled Model Intercomparison Project Phase 7 (CMIP7), we strongly recommend making a greater number

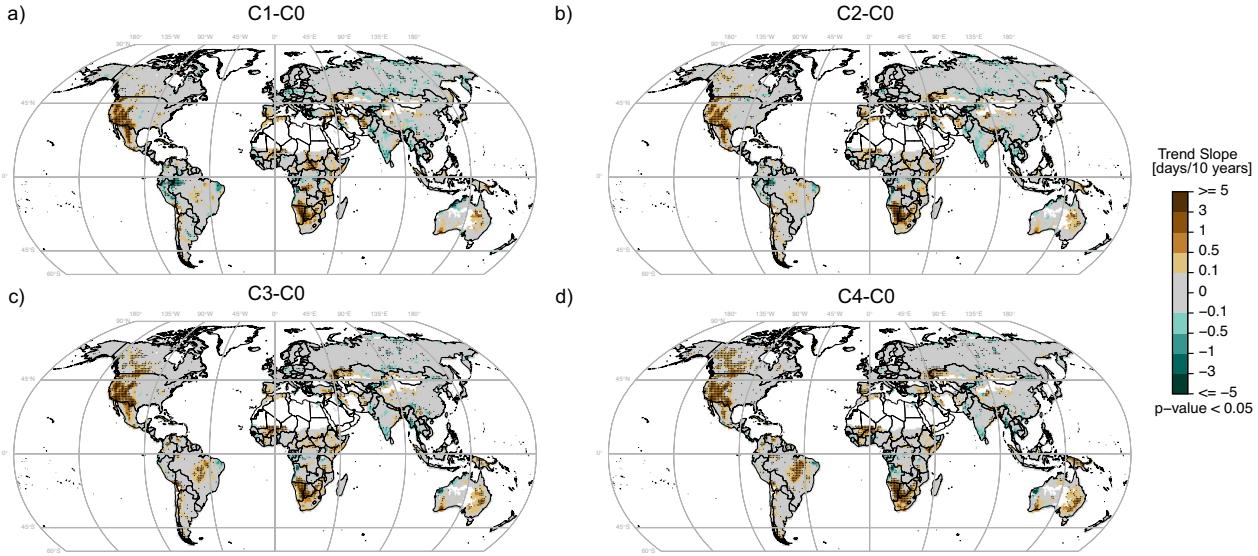

Fig. 3 | Global differences in FWI95d trend estimates using alternative calculation methods compared to baseline (1980–2023). a–d illustrate the difference in trends of days exceeding the 95th percentile Fire Weather Index (FWI95d), calculated using four alternative approximations (C1, C2, C3, and C4) relative to the baseline calculation (C0). Brown colours indicate that the FWI95d trend based on approximations overestimates the FWI95d trend based on the baseline values, while green colours indicate underestimation. Gray colours represent very similar trends (between −0.1 and 0.1 days/10 years). Regions with significant trends (p-value < 0.05) are outlined with black dots.

Table 2 | Areas (million km²) with statistically significant ($p < 0.05$) trend differences from C0

Combination	Significant area (M·km²)
C1	9.76
C2	9.44
C3	11.65
C4	14.82

of key variables available on a sub-daily basis. This would not only enhance the accuracy of FWI assessments but also improve the reliability of climate change impact studies across various sectors.

Previous studies generally agree that the best proxies for calculating the FWI are noon air temperature paired with daily maximum air temperature, and noon relative humidity paired with daily minimum relative humidity—representing the combination we identify as C4[6,7,17]. However, our findings indicate that this combination leads to the highest global overestimation of FWI95d trends, with a 75% increase compared to 65% for the baseline calculation (C0). Moreover, C4 shows the largest area of statistically significant differences, covering approximately 15 million km². Similarly, the combination involving minimum relative humidity (C3) also tends to overestimate FWI trends more than those based on mean relative humidity. Considering these results we recommend the use of combination C1 (which utilizes daily mean values of air temperature, relative humidity, precipitation, and wind speed) for climate change assessments when noon-specific variables are unavailable. An additional advantage of C1 is that it enables the use of a larger number of climate model simulations, as daily mean variables are more commonly available across models and scenarios.

Our findings also highlight the critical role of relative humidity for fire weather trends, especially in regions experiencing sharply declining atmospheric moisture. In such areas, inaccuracies in RH proxies translate directly into exaggerated FWI estimates. Future research should delve deeper into regional-scale dynamics—especially in data-scarce regions like Africa and South America—to refine local wildfire danger assessments. We acknowledge that our analysis relies on ERA5 reanalysis data over a relatively short period (1980–2023). Extending the analysis further back would require substantial reliance on pre-satellite era data, raising additional concerns about data homogeneity and reliability. Additionally, ERA5 itself has known limitations, especially in areas with sparse observational coverage, potentially introducing uncertainty into trend estimations[32]. Nonetheless, several key findings from our study appear robust and generalizable beyond these limitations. For instance, the impact of daily approximations on FWI trends is demonstrably significant, and our analysis clearly indicates that combination C4 (maximum temperature with minimum RH) systematically produces larger trend biases compared to C1 (daily mean values). Although these conclusions are influenced by pronounced changes in specific regions, we find no compelling evidence to favour C4 over C1, particularly as observed trends in temperature (T) and dew point temperature (Td) are broadly consistent with other independent assessments[10]. Furthermore, the enhanced sensitivity of RH to changes in Td and T in regions with declining absolute humidity is not specific to ERA5 alone. Future studies using longer or alternative observational (e.g., the global sub-daily station dataset HadISD[33]) and reanalysis datasets (e.g., MERRA-2[34] and JRA-3Q[35]) would further test the robustness and broader applicability of our conclusions. Additionally, our focus here on the Canadian Fire Weather Index (FWI) is due to its widespread use in both academic research and operational fire-management systems. However, the FWI was originally developed for boreal forests in Canada and may not always be the most appropriate metric for regional studies elsewhere. Other indices, such as the McArthur Forest Fire Danger Index[36] or the Fosberg Fire Weather Index[37], may be preferred and could exhibit different sensitivities to sub-daily meteorological proxies. Although FWI may not optimally capture fire danger in all regions due to local ecological and climatic variability, its widespread use and standardized formulation make it a practical and consistent tool for assessing fire weather trends globally. Future research should investigate whether proxy-induced biases like those documented here also occur in other fire-danger indicators and across diverse ecosystems.

Overall, we underscore the need for caution when using daily approximations for FWI calculations in climate change studies. By highlighting the factors and regions where discrepancies occur, this work contributes toward more accurate modelling of wildfire danger in a changing climate.

Methods

We obtain the Fire Weather Index (FWI) dataset (version 4.1)[15] from the Copernicus Emergency Management Service, which provides global data at

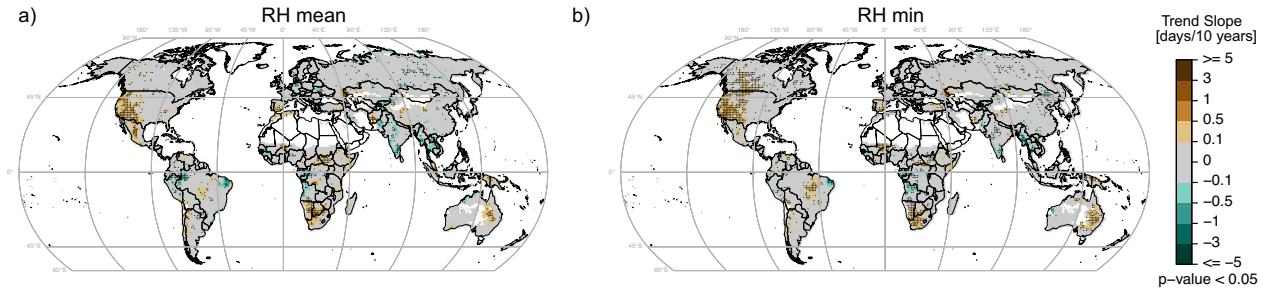

Fig. 4 | Influence of relative humidity proxies. a Trends in differences between FWI95d calculated using daily mean RH instead of noon RH, while maintaining the original FWI definition. **b** Similar to (**a**) but substituting noon RH with daily minimum RH. Regions with significant trend differences (p-value < 0.05) are outlined with black dots.

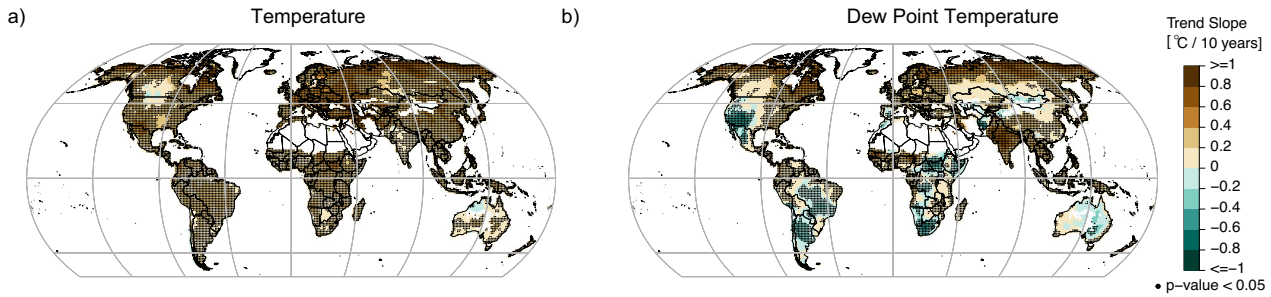

Fig. 5 | Trends in air temperature and dew point temperature from 1980 to 2023 in ERA5. Air Temperature (T) and dew point temperature (Td) were calculated from daily-mean values. **a** Map of the trends in annual mean T. **b** Map of the trends in annual mean Td. Both panels show trend slopes in °C per decade, with significant trends (p-value < 0.05) marked by black dots.

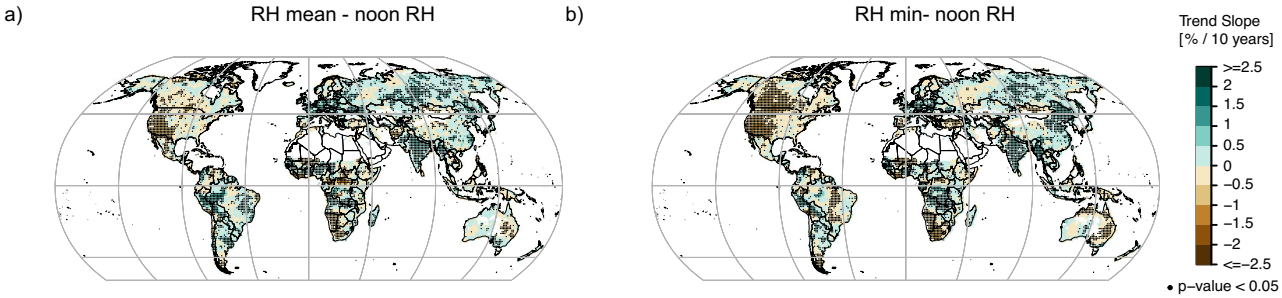

Fig. 6 | Differences in relative humidity trends. a Trends in the differences between RH mean and noon RH over days exceeding the 95th percentile of the Fire Weather Index (FWI). **b** Same as (**a**), but RH min and noon RH. All metrics are based on annual averages over extreme fire danger days. Trends are expressed as percentage change per decade, and only statistically significant trends (p < 0.05) are shown.

a spatial resolution of 0.25° × 0.25° with daily temporal resolution, available at https://ewds.climate.copernicus.eu/datasets/cems-fire-historical-v1 (last accessed 7 June 2025).

To obtain the daily air temperature, relative humidity, precipitation and wind speed values referenced in Table 1, we processed hourly ERA5 data to compute daily minimum, mean, and maximum values. Specifically, for wind speed, we (i) downloaded the hourly 10-meter zonal and meridional wind components (u10 and v10, respectively), and (ii) calculated the daily mean wind speed by averaging the square root of the sum of the squared hourly u10 and v10 components. For relative humidity (RH), we (i) downloaded the hourly 2-meter air temperature, and 2-meter dew point temperature, and (ii) calculated RH using the Magnus formula[38].

Then, we computed the FWI from these daily approximations with the fireDanger R package (v1.1.0; available at https://github.com/SantanderMetGroup/fireDanger; last accessed 7 June 2025). To validate this method for calculating the FWI, we compared our results -obtained using the same input drivers as ref. 15- against the original FWI dataset of ref. 15. The results showed no discernible differences (see Figure. S1), confirming the reliability of this algorithm for estimating the FWI.

We calculated the FWI starting from 1979 but excluded that year to minimize spin-up effects[39], ensuring that initial conditions did not bias our results. Consequently, our analysis covered the 44-year period from 1980 to 2023. For intercomparison at a resolution typical of global climate models, we bilinearly remapped the data from 0.25° to a 1° x 1° grid, consistent with the IPCC AR6 report (https://github.com/SantanderMetGroup/ATLAS/blob/main/reference-grids/; last accessed 7 June 2025). Comparison tests (Figure. S1) confirmed this remapping does not alter our assessment. Following the approach of ref. 7, we apply a mask based on the ESA Climate Change Initiative land cover dataset from 2016[40,41]. Grid cells with >80% bare areas, water, snow/ice, or sparse vegetation are excluded as areas with infrequent burning (shown in white in subsequent maps). To support the research community, we provide two NetCDF datasets available at https://zenodo.org/records/14964973. The first dataset comprises a mask that delineates regions characterized by infrequent fire occurrences at a 1° resolution. The second dataset consists of a mask designed to identify areas where trend biases are present, based on daily approximation methods. The global spatial mean series was obtained through a spatially weighted average based on the cosine of the latitude, which accounts for the decreasing area of grid cells toward the poles.

We assess trends in extreme fire weather by calculating the FWI95d, defined as the annual number of days when fire weather exceeds the 95th percentile of all daily observations for 1980–2023. This metric is chosen because (i) FWI95d focuses on periods of high fire danger when fire growth is more likely (e.g., ref. 42); (ii) many studies have adopted this metric (e.g., refs. 2,7,17); and (iii) as a quantile-based metric, FWI95d minimizes biases in absolute FWI values, enabling a more reliable assessment of trends when using proxies.

We calculated time series slopes via the Theil–Sen estimator[43,44]. We then used the modified Mann-Kendall test for serially correlated data, including the variance correction proposed by Hamed and Rao[45]. All tests employed the mmkh function (modifiedmk package[46]) in R[47]. We applied the False Discovery Rate (FDR) method[48] for multiple testing corrections across the spatial grid.

To determine whether the trend differences between each combination (C1, C2, C3, C4) and the reference dataset (C0) were statistically significant, we followed the same procedure used for the individual time series. Specifically, we (1) computed the difference time series (e.g., C1 – C0), (2) estimated the trend of this difference series using the Theil–Sen estimator, and (3) applied the modified Mann–Kendall test with the Hamed–Rao variance correction to account for serial correlation. We again adjusted for multiple hypothesis testing using the False Discovery Rate procedure. This approach is consistent with ref. 49, where a difference-based test effectively removes the large-scale variability common to both datasets, making it easier to detect subtle differences between their respective trends. In short, we use the same trend estimation (Theil–Sen) and significance assessment (modified Mann–Kendall) for the difference series as we do for the original series. This ensures consistency and robustness in how we quantify and test the significance of the observed trend differences.

Data availability

The datasets used in this study are publicly available. ERA5 hourly variables can be accessed via the Copernicus Climate Data Store at https://cds.climate.copernicus.eu/cdsapp#!/dataset/reanalysis-era5-single-levels. Historical Fire Weather Index data, provided by the Copernicus Emergency Management Service, is available at https://ewds.climate.copernicus.eu/datasets/cems-fire-historical-v1. The global 1 × 1 land-sea mask grid used in this study is available on GitHub at https://github.com/SantanderMetGroup/ATLAS/raw/main/reference-grids/land_sea_mask_1degree.nc4. Global land cover data consistent with the CCI 1992–2015 map series is accessible at https://www.esa-landcover-cci.org/?q=node/197. The same meteorological forcings used to calculate the FWI in Vitolo et al. (2020) are available upon request. While this dataset is not publicly accessible, it is not required to reproduce the main results of this study. Additionally, the code used for the analyses in this study is available upon request from the corresponding author.

Received: 18 March 2025; Accepted: 2 July 2025;
Published online: 28 July 2025

References

1. Taylor, S. W. & Alexander, M. E. Science, technology, and human factors in fire danger rating: the Canadian experience. *Int. J. Wildland Fire* **15**, 121–135 (2006).
2. Jones, M. W. et al. Global and regional trends and drivers of fire under climate change. *Rev. Geophys.* **60**, e2020RG000726 (2022).
3. Van Wagner, C. E. *Development and Structure of the Canadian Forest Fire Weather Index System*. Technical Report 35. Canadian Forest Service, Ottawa, Ontario, Canada (1987).
4. Flannigan, M. et al. Global wildland fire season severity in the 21st century. *Ecol. Manag.* **294**, 54–61 (2013).
5. Herrera, S., Bedia, J., Gutiérrez, J. M., Fernández, J. & Moreno, J. M. On the projection of future fire danger conditions with various instantaneous/mean-daily data sources. *Clim. Change* **118**, 827–840 (2013).
6. Bedia, J., Herrera, S., Camia, A., Moreno, J. M. & Gutiérrez, J. M. Forest fire danger projections in the Mediterranean using ENSEMBLES regional climate change scenarios. *Clim. Change* **122**, 185–199 (2014).
7. Quilcaille, Y., Batibeniz, F., Ribeiro, A. F. S., Padrón, R. S. & Seneviratne, S. I. Fire weather index data under historical and shared socioeconomic pathway projections in the 6th phase of the Coupled Model Intercomparison Project from 1850 to 2100. *Earth Syst. Sci. Data* **15**, 2153–2177 (2023).
8. Jolly, W. M. et al. Climate-induced variations in global wildfire danger from 1979 to 2013. *Nat. Commun.* **6**, 7537 (2015).
9. Bedia, J. et al. Global patterns in the sensitivity of burned area to fire weather: implications for climate change. *Agric. Meteorol.* **214–215**, 369–379 (2015).
10. Gulev, S. K. et al. Changing state of the climate system. In Climate Change 2021: The Physical Science Basis. Contribution of Working Group I to the Sixth Assessment Report of the Intergovernmental Panel on Climate Change [Masson-Delmotte, V. et al (eds.)]. Cambridge University Press, Cambridge, United Kingdom and New York, NY, USA, pp. 287–422, https://doi.org/10.1017/9781009157896.004 (2021).
11. Kalnay, E. et al. The NMC/NCAR 40-year reanalysis project. *Bull. Am. Meteorol. Soc.* **77**, 437–472 (1996).
12. Bowman, D. M. J. S. et al. Vegetation fires in the Anthropocene. *Nat. Rev. Earth Environ.* **1**, 500–515 (2020).
13. Jain, P., Castellanos-Acuna, D., Coogan, S. C. P., Abatzoglou, J. T. & Flannigan, M. D. Observed increases in extreme fire weather driven by atmospheric humidity and temperature. *Nat. Clim. Change* **12**, 63–70 (2022).
14. Jones, M. W. et al. State of wildfires 2023–2024. *Earth Syst. Sci. Data* **16**, 3601–3685 (2024).
15. Vitolo, C. et al. ERA5-based global meteorological wildfire danger maps. *Sci. Data* **7**, 216 (2020).
16. Hersbach, H. et al. The ERA5 global reanalysis. *Q. J. R. Meteorol. Soc.* **146**, 1999–2049 (2020).
17. Abatzoglou, J. T., Williams, A. P. & Barbero, R. Global emergence of anthropogenic climate change in fire weather indices. *Geophys. Res. Lett.* **46**, 326–336 (2019).
18. Dennison, P. E., Brewer, S. C., Arnold, J. D. & Moritz, M. A. Large wildfire trends in the western United States, 1984–2011. *Geophys. Res. Lett.* **41**, 2928–2933 (2014).
19. Abatzoglou, J. T. & Williams, A. P. Impact of anthropogenic climate change on wildfire across western US forests. *Proc. Natl Acad. Sci. USA* **113**, 11770–11775 (2016).
20. Jain, P., Wang, X. & Flannigan, M. D. Trend analysis of fire season length and extreme fire weather in North America between 1979 and 2015. *Int. J. Wildland Fire* **26**, 1009–1020 (2017).
21. Holden, Z. A. et al. Decreasing fire season precipitation increased recent western US forest wildfire activity. *Proc. Natl Acad. Sci. USA* **115**, E8349–E8357 (2018).
22. Turco, M. et al. Anthropogenic climate change impacts exacerbate summer forest fires in California. *Proc. Natl Acad. Sci. USA* **120**, e2213815120 (2023).
23. Trnka, M. et al. Observed and estimated consequences of climate change for the fire weather regime in the moist-temperate climate of the Czech Republic. *Agric. Meteorol.* **310**, 108583 (2021).
24. Hetzer, J., Forrest, M., Ribalaygua, J., Prado-López, C. & Hickler, T. The fire weather in Europe: Large-scale trends towards higher danger. *Environ. Res. Lett.* **19**, 084017 (2024).
25. Jana, S., Gogoi, M. M. & Babu, S. S. Change in precipitation pattern over South Asia in response to the trends in regional warming and free-tropospheric aerosol loading. *Sci. Rep.* **14**, 14528 (2024).
26. Mishra, V. et al. Moist heat stress extremes in India enhanced by irrigation. *Nat. Geosci.* **13**, 722–728 (2020).

27. Willett, K. M., Jones, P. D., Gillett, N. P. & Thorne, P. W. Recent changes in surface humidity: development of the HadCRUH dataset. *J. Clim.* **21**, 5364–5383 (2008).
28. Matsoukas, C. et al. Potential evaporation trends over land between 1983-2008: driven by radiative fluxes or vapour-pressure deficit?. *Atmos. Chem. Phys.* **11**, 7601–7616 (2011).
29. Vicente-Serrano, S. M. et al. Recent changes of relative humidity: regional connections with land and ocean processes. *Earth Syst. Dyn.* **9**, 915–937 (2018).
30. McKinnon, K. A., Poppick, A. & Simpson, I. R. Hot extremes have become drier in the United States Southwest. *Nat. Clim. Change* **11**, 598–604 (2021).
31. Barkhordarian, A., Saatchi, S. S., Behrangi, A., Loikith, P. C. & Mechoso, C. R. A recent systematic increase in vapor pressure deficit over tropical South America. *Sci. Rep.* **9**, 15331 (2019).
32. Soci, C. et al. The ERA5 global reanalysis from 1940 to 2022. *Q. J. R. Meteorol. Soc.* **150**, 4014–4048 (2024).
33. Dunn, R. J., Willett, K. M., Parker, D. E. & Mitchell, L. Expanding HadISD: quality-controlled, sub-daily station data from 1931. *Geosci. Instrum. Methods Data Syst.* **5**, 473–491 (2016).
34. Gelaro, R. et al. The modern-era retrospective analysis for research and applications, version 2 (MERRA-2). *J. Clim.* **30**, 5419–5454 (2017).
35. Kosaka, Y. et al. The JRA-3Q reanalysis. *J. Meteorol. Soc. Jpn. Ser. II* **102**, 49–109 (2024).
36. Noble, I., Gill, A. & Bary, G. McArthur's fire-danger meters expressed as equations. *Aust. J. Ecol.* **5**, 201–203 (1980).
37. Fosberg, M. A. Weather in wildland fire management: the fire weather index, in Proceedings of the Conference on Sierra Nevada Meteorology. 1–4 (1978).
38. Alduchov, O. A. & Eskridge, R. E. Improved Magnus form approximation of saturation vapor pressure. *J. Appl. Meteorol.* **35**, 601–609 (1996).
39. Bedia, J. et al. Seasonal predictions of Fire Weather Index: paving the way for their operational applicability in Mediterranean Europe. *Clim. Serv.* **9**, 101–110 (2018).
40. ESA-CCI. Land Cover CCI Product User Guide Version 2. http://maps.elie.ucl.ac.be/CCI/viewer/download/ESACCI-LC-Ph2-PUGv2_2.0.pdf Accessed 19 December 2024. (2017).
41. ESA-CCI. New release of the C3S global land cover products for 2016, 2017 and 2018 consistent with the CCI 1992–2015 map series. https://www.esa-landcover-cci.org/?q=node/197. Accessed 19 December 2024 (2019).
42. Barbero, R., Abatzoglou, J. T., Steel, E. A. & Larkin, N. K. Modeling very large-fire occurrences over the continental United States from weather and climate forcing. *Environ. Res. Lett.* **9**, 124009 (2014).
43. Theil, H. A rank-invariant method of linear and polynomial regression analysis. *Indag. Math.* **12**, 386–392 (1950).
44. Sen, P. K. Estimates of the regression coefficient based on Kendall's tau. *J. Am. Stat. Assoc.* **63**, 1379–1389 (1968).
45. Hamed, K. H. & Rao, A. R. A modified Mann–Kendall trend test for autocorrelated data. *J. Hydrol.* **204**, 182–196 (1998).
46. Patakamuri, S. K., O'Brien, N. & Patakamuri, M. S. K. Package 'modifiedmk'. Cran. R-project. https://CRAN.R-project.org/package=modifiedmk (2020).
47. R. Core Team. R: A language and environment for statistical computing (R Foundation for Statistical Computing, Vienna, Austria). https://www.R-project.org/ (2023)
48. Benjamini, Y. & Hochberg, Y. Controlling the false discovery rate: a practical and powerful approach to multiple testing. *J. R. Stat. Soc. Ser. B Stat. Methodol.* **57**, 289–300 (1995).
49. Santer, B. D. et al. Statistical significance of trends and trend differences in layer-average atmospheric temperature time series. *J. Geophy. Res.* **105**, 7337–7356 (2000).

Acknowledgements

The authors wish to acknowledge the anonymous reviewers for their detailed and helpful comments to the original manuscript. This work was supported by the project 'Climate and Wildfire Interface Study for Europe (CHASE)' under the 6th Seed Funding Call by the European University for Well-Being (EUniWell). M.T. acknowledges funding by the Spanish Ministry of Science, Innovation and Universities through the Ramón y Cajal Grant Reference RYC2019-027115-I and through the project ONFIRE, Grant PID2021-123193OB-I00, funded by MCIN/AEI/10.13039/501100011033 and by "ERDF A way of making Europe". A.P. acknowledges the support of the EU H2020 project "FirEUrisk", Grant Agreement No. 101003890. Y.Q. acknowledges the support of the EU Horizon Europe project SPARCCLE, Grant Agreement No. 101081369. RJHD was supported by the Met Office Hadley Centre Climate Programme funded by DSIT. C.A-M. received funding from the PROMETEO Ref. CIPROM/2023/38. A.F.S.R. acknowledges the Alexander von Humboldt Foundation (AvH) for a postdoctoral fellowship and the Deutsche Forschungsgemeinschaft (DFG) - Project number 530175554. J.B. has received research support from Grant PID2023-149997OA-I00 (PROTECT Project) funded by MICIU/AEI/10.13039/501100011033 and by ERDF/EU.

Author contributions

A.M. and M.T. conceived the study and drafted the manuscript. A.M., G.G.-M., A.Mo., and M.A.T.V. performed the data analysis and prepared the figures. All authors reviewed and approved the final manuscript.

Competing interests

The authors declare no competing interests.

Additional information

Supplementary information The online version contains supplementary material available at https://doi.org/10.1038/s41612-025-01163-0.

Correspondence and requests for materials should be addressed to Marco Turco.

Reprints and permissions information is available at http://www.nature.com/reprints

Publisher's note Springer Nature remains neutral with regard to jurisdictional claims in published maps and institutional affiliations.

Open Access This article is licensed under a Creative Commons Attribution-NonCommercial-NoDerivatives 4.0 International License, which permits any non-commercial use, sharing, distribution and reproduction in any medium or format, as long as you give appropriate credit to the original author(s) and the source, provide a link to the Creative Commons licence, and indicate if you modified the licensed material. You do not have permission under this licence to share adapted material derived from this article or parts of it. The images or other third party material in this article are included in the article's Creative Commons licence, unless indicated otherwise in a credit line to the material. If material is not included in the article's Creative Commons licence and your intended use is not permitted by statutory regulation or exceeds the permitted use, you will need to obtain permission directly from the copyright holder. To view a copy of this licence, visit http://creativecommons.org/licenses/by-nc-nd/4.0/.

© The Author(s) 2025